Visible photoluminescence from porous *a*-Si:H and porous *a*-Si:C:H thin films

M. J. Estes,[a] L. R. Hirsch, S. Wichart, and G. Moddel
Department of Electrical and Computer Engineering and the Optoelectronic Computing Systems Center, University of Colorado, Boulder, Colorado 80309-0425

D. L. Williamson
Department of Physics, Colorado School of Mines, Golden, Colorado 80401

(Received 26 July 1996; accepted for publication 23 May 1997)

We report on the influence of doping, temperature, porosity, band gap, and oxidation on the photoluminescence (PL) properties of anodically etched porous *a*-Si:H and *a*-Si:C:H thin films. Only boron-doped, *p*-type *a*-Si:H samples exhibited visible photoluminescence. Two broad PL peaks at ~1.6 and ~2.2 eV are apparent in room temperature PL spectra. The intensity of the 2.2 eV peak as well as the nanovoid density in the unetched *a*-Si:H layers both correlate well with boron concentration. We see evidence of discrete defect or impurity levels in temperature-dependent luminescence measurements, where we observe multiple luminescence peaks. Unlike in porous crystalline silicon, the luminescence energy in porous amorphous silicon does not change with porosity. We do, though, observe a correlation of luminescence energy with band gap of the starting *a*-Si:C:H films. Oxidation, either native or anodic, reduces photoluminescence intensity. We discuss the implications of these observations on the nature of the luminescence mechanism. © *1997 American Institute of Physics.* [S0021-8979(97)07716-5]

I. INTRODUCTION

We have investigated the visible photoluminescence (PL) properties of anodically etched porous films of hydrogenated amorphous silicon (*a*-Si:H) and, for the first time, amorphous silicon carbide (*a*-Si:C:H). Our observations partly confirm the results of Bustarret *et al.*,[1–3] who first reported on room temperature visible luminescence from porous *a*-Si:B:H films formed by anodic etching in ethanoic HF solution. In a similar study, Lazarouk *et al.*[4] reported red light emission from phosphorous-doped *n*-type *a*-Si:H pillar structures anodized in 1% aqueous HF at 2 mA/cm^2.[2] It is not clear whether the anodization of the pillar structures resulted in formation of a porous layer or in size reduction and passivation of the *a*-Si:H pillars. Others have also reported the formation of porous amorphous silicon, albeit without light emission, by anodic etching[5,6] and chemical stain etching.[3,7,8] One of the major outcomes of these studies was the realization that crystallinity is not necessary for visible light emission from silicon nanostructures.

As a result, quantum confinement should not be a factor in the higher than expected luminescence energy from porous *a*-Si:H. This conclusion may also have ramifications in porous crystalline silicon, where very similar red-orange light emission is observed.[1,4] A number of theories, which do not involve quantum effects, have been proposed to explain the visible luminescence. These include light emission from: (1) surface molecular agents such as siloxene[9] or polysilanes,[10] (2) oxide defect centers,[11,12] and (3) amorphous silicon oxynitride alloys.[13] In addition, we recently proposed that a theory of size-dependent luminescence in amorphous semiconductors, which was based on a model originally proposed by Tiedje *et al.*,[14,15] may partly explain the luminescence from amorphous silicon nanostructures and possibly even porous crystalline silicon.[16] The recent results of Lu *et al.*,[17] who reported on size-dependent PL from *a*-Si/*a*-SiO_2 multilayers formed by molecular beam epitaxy, may support this theory. Although Lu *et al.* presented a strong case for quantum confinement in their samples, we believe that quantum confinement effects in amorphous silicon nanostructures are small due to the short coherence length of free carriers in the material. At present, no clear picture has emerged of the luminescence process(es) in porous *a*-Si:H; this is partly because little experimental data is available and partly because it is difficult to distinguish between models using standard experimental techniques.

The purpose of our study was to gain a better understanding of the properties and mechanisms of the light emission from porous *a*-Si:H. Toward this end, we investigated the effects of doping, temperature, porosity, band gap, and oxidation on the photoluminescence properties of porous *a*-Si:H and *a*-Si:C:H films. We etched *n*-type, *p*-type, and intrinsic *a*-Si:H layers and examined the effects of doping type and concentration on both etching and PL characteristics. We show that boron plays a key role in this regard. We measured PL spectra at temperatures between 83 and 300 K and found evidence of defect-related PL. By varying anodic etching conditions, we produced porous layers with a range of porosities to examine the possible size effects in the PL emission energy. Unlike in porous crystalline silicon, we found no correlation of PL energy with porosity. We also produced a series of *a*-Si:C:H films and show a clear correlation between band gap and PL energy. Finally, we examined the effects of oxidation, both environmental and anodic, on the PL from porous *a*-Si:H layers. Oxidation universally reduced PL intensity in our samples. We discuss the impli-

[a]Current address: Avionics Directorate, Wright Laboratory, Wright-Patterson AFB, OH 45433.

 0021-8979/97/82(4)/1832/9/$10.00

TABLE I. Deposition parameters, band gaps, and conductivities of the series of doped *a*-Si:H films used in this study. The columns under flows are for the atomic flow rates of the active atoms in the deposition gases used: silane (Si), 1% trimethylboron in helium (B), phosphine (P), and hydrogen (H_2).

Film	Type	Flows (sccm) Si	B	P	H_2	Pressure (mT)	rf power density (W/cm^2)	Tauc band gap (eV)	Conductivity (Ω^{-1} cm^{-1})
95-44	p^{++}	5	0.2	0	45	300	0.079	1.62	1.6×10^{-6}
95-30	p^{+}	30	0.3	0	0	500	0.016	1.75	2.1×10^{-5}
95-35	p^{-}	40	0.04	0	0	300	0.016	1.75	1.0×10^{-6}
95-36	i	40	0	0	0	500	0.016	1.76	8.0×10^{-10}
95-37	n^{+}	40	0	0.4	0	300	0.016	1.69	7.9×10^{-3}

cations of our experimental results on the etching and luminescence processes in porous *a*-Si:H.

II. EXPERIMENT

We deposited hydrogenated amorphous silicon (*a*-Si:H) films by plasma enhanced chemical vapor deposition (PECVD) at a plasma frequency of 13.56 MHz and a substrate temperature of 210 °C. Plasma power density was 15.7 mW/cm^2. We used SiH_4 as the source gas and added dopant gases of PH_3, $B(CH_3)_3$, and CH_4 to produce *n*-type, *p*-type, and carbon-alloyed *a*-Si:H layers, respectively. Films of thickness 1 to 2 μm were deposited onto polished (111) silicon (*p*-type, 1–20 Ω cm), indium-tin oxide (ITO) coated glass, and Corning 7059 glass substrates. For successful anodization, we found that the *a*-Si:H films had to adhere well to the substrate, have low built-in stress, and have low pinhole density. Thus, substrate surface cleanliness and proper deposition conditions were key factors. To provide electrical contact for anodization, we evaporated aluminum onto the backs of the silicon substrates and applied silver paint to the corners of the ITO/glass substrates.

To form the porous layer, we anodically etched the *a*-Si:H in solutions of HF:H_2O:ethanol using an *o*-ring sealed teflon etching cell and Pt wire anode. We anodized the samples with etching current densities of 0.1–30 mA/cm^2 until 0.9 C of charge had been exchanged (typical conditions were 1 mA/cm^2 for 15 min in 1:1:2 HF:H_2O:ethanol). After anodization, we rinsed the films in ethanol and allowed them to air dry.

We used the 365 nm line of a 200 watt mercury arc lamp as the excitation source for PL measurements. The optical power illuminating the sample was approximately 0.1 mW over an area of roughly 1 mm by 3 mm. Samples were mounted in a liquid nitrogen cryostat. The PL light was detected through a 1/8 m spectrometer with a spectral bandwidth of 16 nm at 500 nm wavelength using a photomultiplier tube (PMT) or a silicon photodiode. We used 450 nm low pass filters to keep the 365 nm excitation light from reaching the detector. All PL spectra were corrected for instrument response, although the correction for the PMT detector data between 1.4 and 1.5 eV was slightly inaccurate and yielded smaller than actual PL intensities.

To characterize the nanostructure of the as-deposited *a*-Si:H, we measured small-angle x-ray scattering (SAXS) on a series of films with increasing boron content deposited on thin (70 μm) *c*-Si. Identical deposition conditions were used to those for the series of films listed in Table I (i,p^-,p^+,p^{++}). The SAXS measuring techniques and data analysis are described in detail elsewhere.[18]

III. RESULTS

A. Doping dependence

We prepared a series of five *a*-Si:H films to investigate the effects of doping on the etching and luminescence properties of our *a*-Si:H. These samples included p^{++}, p^+, p^-, i, and n^+-doped films. We list the deposition parameters and resulting Tauc band gaps[19] and conductivities in Table I. Except as noted, all the *a*-Si:H samples used in this experiment were deposited on (111)Si substrates. Under the deposition conditions used for these films, we expect the film structure to be completely amorphous. Film No. 95-44 in Table I was an effort to approximately reproduce the film stoichiometry of Bustarret *et al.*,[1] whose films appear to have a very high boron concentration.

Boron-doped *a*-Si:H films etched quite readily in 25% ethanoic HF. The resulting porous layer in highly doped p^+ films was smooth and specular, showing uniform interference colors. More lightly doped *p*-type films also showed interference colors, but the surfaces were rough and optically diffuse. We could obtain a porous layer from the highly boron-doped No. 95-44 film only by anodic etching in 50% aqueous HF at 1 mA/cm^2. Lower HF concentrations or higher etching currents resulted in electropolishing (uniform, nonporous etching, not necessarily shiny and smooth). We found that while the p^+ and p^- samples yielded porous layers over a wide range of HF concentrations and etching currents, *n*-type and intrinsic films required strong white-light illumination in excess of AM1 ($\sim$100 mW/cm^2) intensity to produce porous layers with 25% HF solution and 1 mA/cm^2 etching current. Even so, the resulting porous films from the i and n^+ samples were black and very diffuse indicating strong light scattering and absorption, presumably due to larger feature sizes than for the *p*-type films. We also attempted to etch *n*-type *a*-Si:H films in 1% aqueous HF as did Lazarouk *et al.*,[4] however, the resulting surfaces showed no signs of visible PL. In terms of uniformity and adherence, the porous layers formed on the (111)Si substrates were notably superior to those formed on ITO/glass substrates.

While we consistently obtained weak blue light emission from stain-etched p^+ *a*-Si:H films, we found no trace of red PL in these spectra. These findings, coupled with our previous efforts with stain-etched microcrystalline silicon films,[20]

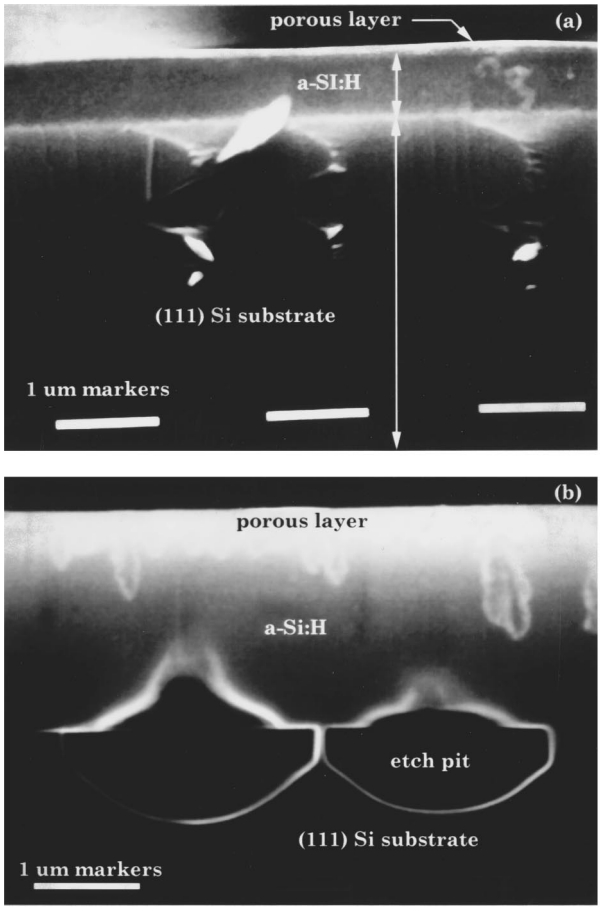

FIG. 1. Scanning electron micrographs of the cross sectional views of (a) porous p^+a-Si:H and (b) porous p^-a-Si:H. The images clearly show the top porous layers, which appear white, and the remaining unetched a-Si:H films, which appear gray. The p^+ porous layer in (a) etched smoothly and uniformly but only a thin $\sim$800 Å porous layer remained after rinsing. The p^- porous layer appears very rough and nonuniform and is thicker than the p^+ layer. The horizontal white bars on the scale at the bottom of the images correspond to 1 μm.

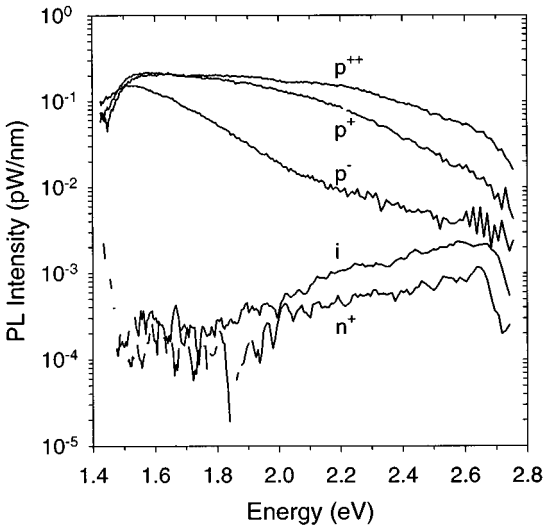

FIG. 2. Room temperature porous a-Si:H photoluminescence intensity (log scale) as a function of doping. The porous layers were formed 25% ethanoic HF (50% aqueous HF for the p^{++} layer) at 1 mA/cm^2. The i and n^+ samples were etched under strong white light illumination.

lead us to conclude that crystallinity is a prerequisite for the red-orange light emission from stain-etched films. It may be that either the morphologies of the stain-etched and anodized films are significantly different or that the two etching processes lead to different radiative processes.

In Figs. 1(a) and 1(b), we show scanning electron microscope cross sectional images of porous a-Si:H layers on (111) Si. In Fig. 1(a), the uniformly etched porous layer of a p^+ sample, etched at 1 mA/cm^2 in 25% HF, is evident as the white top layer of thickness $\sim$0.08 μm while the remaining a-Si:H film of thickness $\sim$0.58 μm and the crystalline silicon substrate below show up as grey. The initial a-Si:H film was $\sim$2.15 μm; we believe that the remaining top portion of the film disintegrated during the ethanol rinse as the film color changed during rinsing. In Fig. 1(b), we see the much rougher porous layer produced on a p^- sample at 30 mA/cm^2 in 25% HF. The p^- samples did not seem to have the film disintegration problems of the p^+ layers. As is evident in Fig. 1(b) this particular sample had a large number of pinholes that etched through the a-Si:H film to the (111) Si substrate below. These etch pits do not appear to affect the luminescence of the sample as the 365 nm light is completely absorbed by the remaining a-Si:H layer before reaching the substrate. Porous a-Si:H layers formed on ITO/glass substrates exhibited nearly identical PL to that from layers on crystalline silicon substrates, clearly demonstrating that the light emission does not come from etch pits in crystalline silicon substrates.

We recorded the room temperature PL spectra of the p^{++} (95-44), p^+ (95-30), p^- (95-35), i (95-36), and n^+ (95-37) doped layers using a photomultiplier detector and show these data in Fig. 2. The data have been normalized to the instrument response. Only the boron-doped films yielded detectable red-orange luminescence. The blue components to the PL spectra from these films seem to be real (from the porous silicon), though we cannot rule out the possible presence of organic contaminants from the etching that could be the source of this light. The spectrum resembles previously reported PL of porous a-Si:B:H (Ref. 1) with a room temperature peak energy near 1.6 eV and full-width at-half-maximum (FWHM) of about 0.8 eV. Also evident in these spectra are weak peaks at $\sim$1.9 and $\sim$2.2 eV that seem to increase in intensity with boron concentration. The intensity of the $\sim$1.5–1.6 eV peak does not appear to have a correlation with boron concentration other than the fact that it is present only in boron-doped films. We estimate our room temperature PL efficiencies to be 0.01%–0.1%. In fact, the dim orange-colored PL from these samples was just barely visible to the eye in a darkened room. Bustarret *et al.*[3] reported 2%–5% external quantum efficiencies from their porous a-Si:H films; however, these high efficiencies only occurred on microscopic features on the surface of the porous films. Macroscopic quantum efficiencies were considerably lower.[21]

In Fig. 3, we show the 83 K PL spectra of the p^{++}, p^+, p^-, and i layers. We recorded these data, which were approximately 40 times more intense than the room tempera-

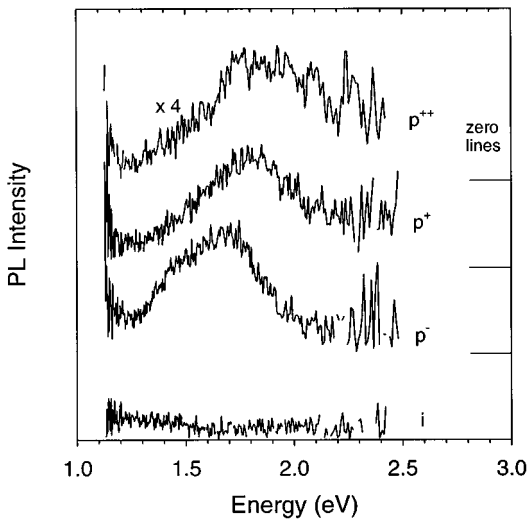

FIG. 3. 83 K photoluminescence spectra of the porous a-Si:H layers of Fig. 2 showing the effect of boron concentration. The n^+ sample did not exhibit any detectable PL at low temperature. The curves have been displaced along the y axis for clarity.

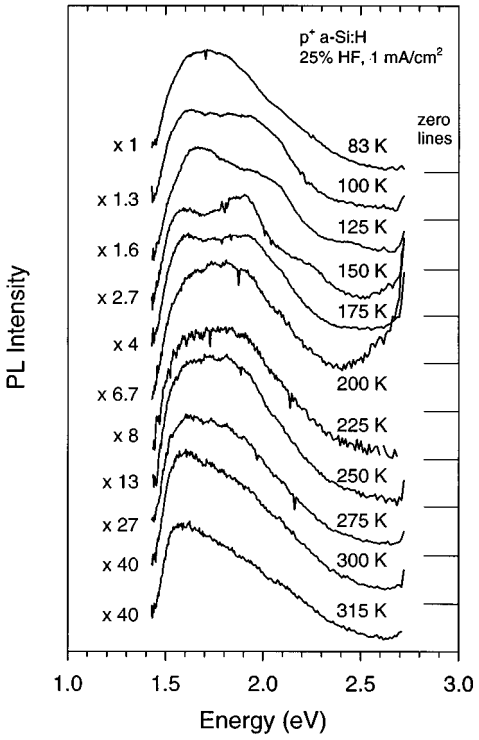

FIG. 4. Temperature dependence of the photoluminescence spectrum of a p^+ porous a-Si:H etched at 1 mA/cm^2 for 15 min in 25% HF. The curves have been displaced as indicated for clarity. The structure in the 100–175 K PL spectra may result from defect or impurity level transitions.

ture PL signals, using a silicon photodiode detector so that we could observe the low energy tail of the PL peaks. Unfortunately, the silicon photodiode was much noisier than the PMT used for Fig. 2. The very weak visible PL from the undoped i layer appears to be real, though this film probably has some residual boron contamination from the previous p-type deposition run. The n-type sample had no detectable photoluminescence at 83 K. The low temperature luminescence peak energy shifts to higher energies as the boron concentration increases, with peaks at $\sim$1.7, 1.8, and 1.9 eV for the p^-, p^+, and p^{++} samples, respectively. A subtle blue shift of the 1.5–1.6 eV peak is also evident in the room temperature data of Fig. 2, where we find peak energies of $\sim$1.52, 1.55, and 1.60 eV for the p^-, p^+, and p^{++} samples, respectively.

B. Temperature dependence

The temperature dependence of the photoluminescence spectrum of a p^+ sample etched at 1 mA/cm^2 in 25% HF, shown in Fig. 4, reveals some remarkable structure that appears in the intermediate temperature range between 100 and 175 K. These peaks are not interference fringes, as they change dramatically with temperature, but rather are consistent with the presence of multiple radiative processes with strong temperature dependencies. Assuming that quantum confinement effects are not present in the amorphous nanostructures, this data would seem to be the strongest indication of defect- or impurity-related radiative transitions since the peaks are relatively sharp. Careful study of these spectra reveals four emission peaks at $\sim$1.60, 1.90, 2.05, and 2.25 eV whose peak energies do not change appreciably with temperature. The broad, single-peaked spectra (at $T=83$ K, for example) appear to be made up of multiple unresolved PL lines. The blue emission between 150 and 200 K also appears to be real, though it seems odd that it would disappear so dramatically between 200 and 225 K. The rapid falloff in PL between 1.4 and 1.5 eV in these spectra is due to inaccurate normalization of the PMT detector signal at the edge of the detector response.

In Fig. 4, we see that the PL intensity drops by roughly a factor of 40 between 83 K and room temperature. The 1.3–1.4 eV luminescence in undoped a-Si:H, on the other hand, decreases by more than 1000 times in the same temperature range.[22] Although the structure in the PL complicates the issue, the overall trend in our porous a-Si:H samples appears to be a redshift with increasing temperature.

C. Etching dependence

In porous crystalline silicon, the trend of increasing luminescence energy with increasing porosity is fairly well established.[23,24] Higher porosity films may be produced by increasing etching current density and by decreasing etchant HF concentration. This correlation suggests, at least indirectly, a size dependence of the PL. In porous a-Si:H, we see no such trend in the PL.

We show the room temperature PL spectra of five p^+ porous layers as a function of HF concentration in Fig. 5. The effective indices of refraction for the top porous layers were measured with an ellipsometer at 632 nm wavelength and are given next to each curve. The effective index of refraction is an indication of layer porosity through the effective medium treatment.[25] Thus, while decreasing HF concentration does indeed produce layers of increasing porosity in a-Si:H, this effect does not bring about a shift in peak luminescence energy. The high energy PL tail, however,

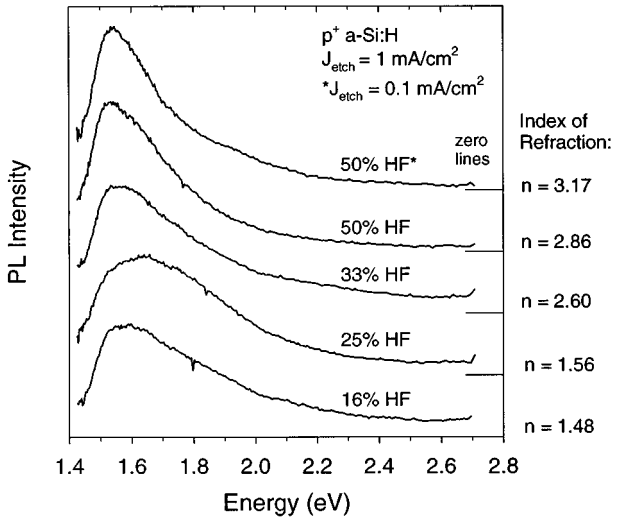

FIG. 5. Room temperature photoluminescence spectra showing the effect of HF concentration on porosity and PL. In contrast to porous *c*-Si, no correlation appears to exist between PL energy and porosity. The numbers on the right hand side of the graph indicate the measured refractive index of the porous layer. These data are from p^+ porous *a*-Si:H samples etched as indicated above each curve.

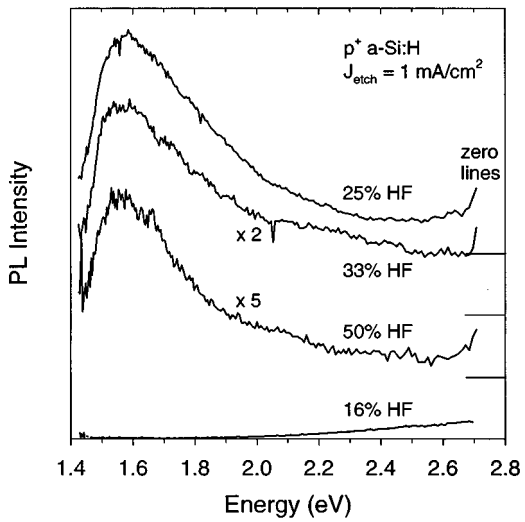

FIG. 7. Room temperature photoluminescence spectra of p^+ porous *a*-Si:H layers on ITO/glass substrates. The data is similar to that in Fig. 5 except for substrate type. These curves clearly show that the PL emanates from the porous *a*-Si:H.

does appear to increase very slightly with porosity. We do not know why the peak energy of the sample etched in 25% HF is at a higher energy ($\sim$1.65 eV) than in all the other spectra. In Fig. 6, we plot the spectra of three samples etched at current densities ranging from 0.316 to 31.6 mA/cm^2. Clearly, current density has little effect on porosity and no effect on PL.

As proof that the visible PL from our samples originates from the porous *a*-Si:H and not from porous crystalline silicon in the substrate [such as etch pits in Fig. 1(b)], we prepared porous *a*-Si:H films on indium-tin-oxide (ITO) coated glass substrates. In Fig. 7, we show that PL spectra for four such samples etched at 1 mA/cm^2 for 15 min in etchants with 16%, 25%, 33%, and 50% HF concentrations. The spectra are similar to those of Fig. 5 with the exception that the ITO sample etched in 16% solution had no red PL. Because the ITO samples are on transparent substrates, we were able to measure absorbance from the porous layers, which we illustrate in Fig. 8. We find an absorbance shoulder at $\sim$1.6 eV in the 50% and 33% HF curves that may be associated with the $\sim$1.6 eV PL peak.

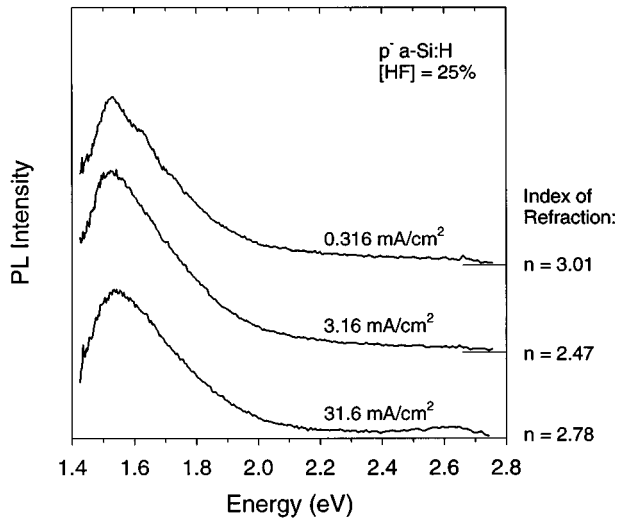

FIG. 6. Room temperature photoluminescence spectra showing the effect of etching current density on layer porosity and PL. The graph shows that etching current, over two orders of magnitude, does not affect PL. The numbers on the right hand side are the effective indices of refraction for the porous layers, which were formed on p^- samples in 25% HF.

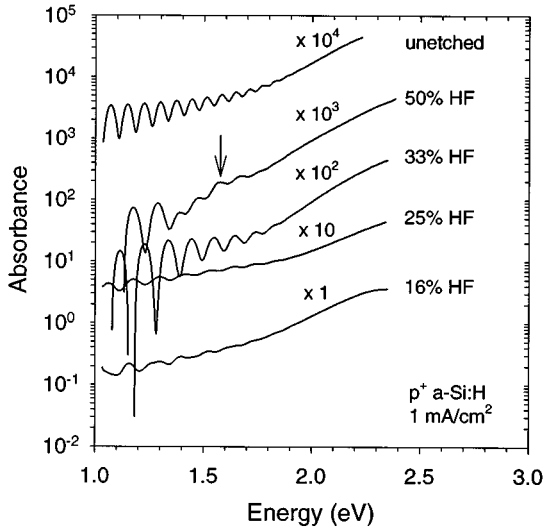

FIG. 8. Comparison of the absorbance of the porous *a*-Si:H layers of Fig. 7 with that of the unetched p^+*a*-Si:H. The curves have been displaced along the log-*y* axis by multiplying successive traces by factors of 10. An absorbance shoulder at $\sim$1.6 eV can be seen in the porous films etched in 50% and 33% HF solutions.

TABLE II. Deposition parameters, band gaps, and conductivities of the series of doped *a*-Si:C:H films used in this study. The data in the gas flow columns are for the atomic flows of the active atoms in the deposition gases used: silane (Si), methane (C), and 1% trimethylboron in helium (B).

Film	Type	Flows (sccm) Si	C	B	Pressure (mT)	rf power density (W/cm^2)	Tauc band gap (eV)	Conductivity (Ω^{-1} cm^{-1})
95-30	p^+	30	0	0.3	500	0.016	1.75	2.1×10^{-5}
95-43	p^+	8	12	16	300	0.016	1.90	1.3×10^{-6}
95-42	p^+	8	24	16	300	0.016	2.00	6.5×10^{-8}
95-41	p^+	8	40	16	300	0.016	2.13	2.9×10^{-9}
95-40	p^+	5	40	5	300	0.024	2.25	3.5×10^{-10}

D. *a*-Si:C:H alloys

By adding carbon during the PECVD deposition process, we produced a series of *a*-Si:C:H films with band gaps ranging from 1.75 to 2.25 eV. The ability to control band gap is unique to the amorphous case as one cannot adjust the band gap of the starting material in porous crystalline silicon. In Table II, we list the deposition parameters, Tauc band gaps, and conductivities of this series of films. An unfortunate side effect of increased carbon content was a rapid decrease in conductivity. Thus, the wider band gap *a*-Si:C:H films were more difficult to anodize than the lower carbon content films, as etching became very sensitive to pinholes in the high resistivity films.

In Fig. 9, we show the 83 K PL spectra of three films (Nos. 95-30, 95-43, 95-42 of Table II) etched at 1 mA/cm^2 in 25% ethanoic HF. The PL from these porous *a*-Si:C:H samples, which had Tauc band gaps of 1.75, 1.90, and 2.0 eV, peak at approximately 1.7, 1.9, and 2.1 eV, respectively. Thus, we see a clear correlation between band gap and luminescence energy. In Fig. 10, we plot the room temperature PL spectra of a series of porous *a*-Si:C:H layers etched at 1 mA/cm^2 in 50% aqueous HF. Etchants with HF concentrations below 50% tended to etch through pinholes in the samples with high carbon concentrations and thus did not yield porous layers. The structure in the PL spectra of Fig. 10 may be due in part to interference fringes; however, given the results of the temperature-dependence measurements of Fig. 4, we cannot rule out the possibility that it may again indicate the presence of discrete energy levels in the radiative process. While this structure makes quantitative comparison of peak PL energies difficult to compare, it is apparent from the graph that the average PL energy increases with band gap of the starting material. The width of the PL spectra also appears to increase with increasing carbon content, consistent with greater bond disorder within the wide band gap *a*-Si:C:H.

E. Aging

In the cases of porous crystalline silicon[26] and porous amorphous silicon[1] previously reported, postelectrooxidation of the porous layer resulted in a significant increase of the PL intensity. For our porous *a*-Si:H films, however, anodic oxidation in 0.1 M KNO_3 at 1 mA/cm^2 caused a decrease in intensity and a blueshift of PL energy, as shown in Fig. 11 for the No. 95-44 p^{++} sample. Oxidation for too long a time resulted in crazing and lift off of the porous

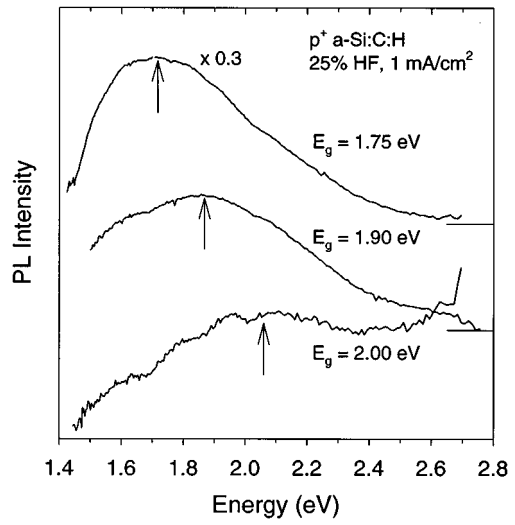

FIG. 9. 83 K photoluminescence spectra of porous *a*-Si:C:H films etched at 1 mA/cm^2 in 25% HF. The Tauc band gaps of the *a*-Si:C:H layers before etching are given by each spectrum. Arrows under each curve indicate the approximate PL peak position, which correlates well with the band gap of the starting layer.

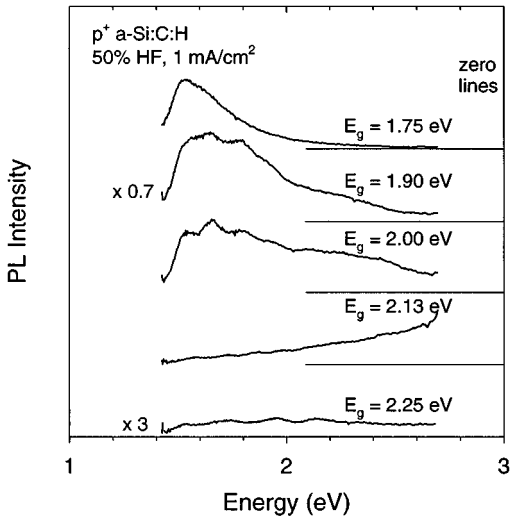

FIG. 10. Room temperature photoluminescence spectra of porous *a*-Si:C:H layers as a function of C concentration. The samples were etched at 1 mA/cm^2 in 50% aqueous HF. The Tauc band gaps of the *a*-Si:C:H layers before etching are listed above each curve. The data exhibit a trend of increasing photoluminescence energy with increasing band gap energy.

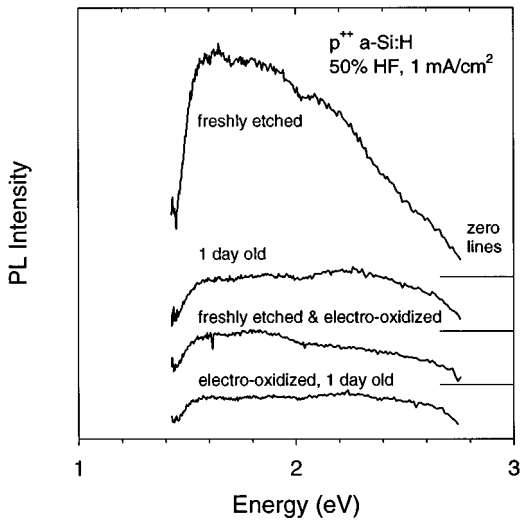

FIG. 11. Room temperature photoluminescence showing aging effects on anodized p^{++} porous layers. The films were etched at 1 mA/cm^2 in 50% HF for 15 min. The electro-oxidized film was subsequently anodized in 0.1 M KNO_3 for 60 s. The sample type and age of the sample at the time the PL was taken are indicated on the graph.

layer. We compare the effects of exposure to ambient atmosphere for the electro-oxidized and unoxidized samples in Fig. 11, where the PL for the freshly etched and 1 day old samples are shown. Air exposure did not seem to degrade and broaden the PL of the more lightly boron-doped films (Nos. 95-30 and 95-35) nearly as much as it did for No. 95-44 in Fig. 11.

IV. DISCUSSION

Previously, we examined the effect of structure size on the predicted PL from *a*-Si:H nanostructures.[16] Using this model, we calculated the PL spectrum from a uniform size distribution of *a*-Si:H spheres with diameters from 10 Å to 1 μm. The model predicts a broad, temperature-insensitive PL peak centered at $\sim$1.65 eV with a long high energy tail. We expect that porous *a*-Si:H similarly comprises clusters of *a*-Si:H with a range of sizes down to the nanometer scale. However, the appearance of multiple PL peaks in the temperature-dependent PL spectra (Fig. 4) and in the doping-dependent PL spectra (Fig. 2) is more consistent with radiative transitions through discrete defect or impurity levels. This type of structure is at odds with the broad, featureless band-tail luminescence predicted by our model and seen in ''bulk'' *a*-Si:H (Ref. 27) and *a*-Si:O_x:N_y:H.[13] From the aging data of Fig. 11, we may also infer that multiple PL processes are occurring in porous *a*-Si:H as oxidation strongly reduces the $\sim$1.6 eV peak while only slightly reducing the $\sim$2.2 eV luminescence. Multiple PL peaks have been observed in porous crystalline silicon as well[28,29] and have been cited[29] as evidence for luminescence centers in SiO_x, such as the nonbridging oxygen hole center.[12]

In the luminescence center model of porous silicon, absorption of excitation light is thought to occur in quantum confined silicon nanocrystals. Photoexcited electrons and holes then recombine through oxide defect states on the surfaces of the nanocrystals.[30] In porous amorphous silicon, we do not expect quantum confinement effects, and therefore carrier injection into high energy surface states must result from another mechanism. Assuming that photocarriers are generated in the internal amorphous silicon nanostructures, then possible carrier injection paths may be through hot carrier tunneling into surface radiative states[31] or through an effective widening of the mobility gap in *a*-Si:H.[28] While these results are in apparent contradiction to our model of size-dependent *a*-Si:H PL, if carriers in the *a*-Si:H conduction and valence bands are trapped in radiative surface states faster than they can recombine within the *a*-Si:H, then surface state recombination will dominate.

As we have shown, one can produce porous *a*-Si:H layers of differing porosities by varying etching current density and HF concentration. However, the photoluminescence spectra of the resulting samples remains nearly constant, with a room temperature PL peak energy of $\sim$1.6 eV; even the PL intensity remains relatively constant. This result is in marked contrast to what is observed in porous crystalline silicon, where PL energy increases with porosity. In the quantum confinement model, the blue shift of the PL with porosity is assumed to be due to an overall shrinking of crystallite size. In the oxide defect model, Prokes has proposed that the blue shift is caused by added bond strain as oxide forms around silicon structures with smaller radius of curvature.[32] If this was the case, then one would expect the same blue shift in porous *a*-Si:H. Therefore, either the PL energy in porous *a*-Si:H is independent of feature size or the size of the remaining amorphous silicon skeleton is self-limited (only the porosity changes with etching variations). Self-limiting of the remaining *a*-Si:H wires in porous *a*-Si:H could arise from an effective widening of the mobility gap in *a*-Si:H nanowires[28] or from surface trapping of charge carriers.

We know of no evidence linking porosity with nanostructure size in porous *a*-Si:H. Bustarret *et al.* have suggested that feature size in porous *a*-Si:H may be determined by available percolation paths for etching current in the *a*-Si:H.[1] If so, then a higher boron concentration may result in a higher density of percolation paths and consequently smaller nanostructures in the resulting porous layer. Indeed, as we show in Figs. 3 and 4, the PL peak energy does increase slightly with boron concentration. In addition, from small angle x-ray scattering results, we find a correlation of nanovoid density with boron concentration in our unetched *a*-Si:H films. We plot the PL intensity of porous layers with different boron concentrations versus the measured nanovoid density of unetched *a*-Si:H films in Fig. 12. Our undoped films have a density of approximately spherical nanovoids of 1.2×10^{16} cm^{-3} (average void separation $\sim$55 nm) with an average diameter $\sim$4 nm while our p^{++} films have a nanovoid density of 4.0×10^{19} cm^{-3} (average void separation $\sim$4 nm) with an average diameter $\sim$1.0 nm. The correlation between boron concentration and nanovoid density is nearly 1:1, indicating that each B atom probably leads to a nanovoid. Pore formation during anodic etching may be seeded at nanovoids or may occur preferentially at nanovoids. This behavior would explain why the surface morphology of the

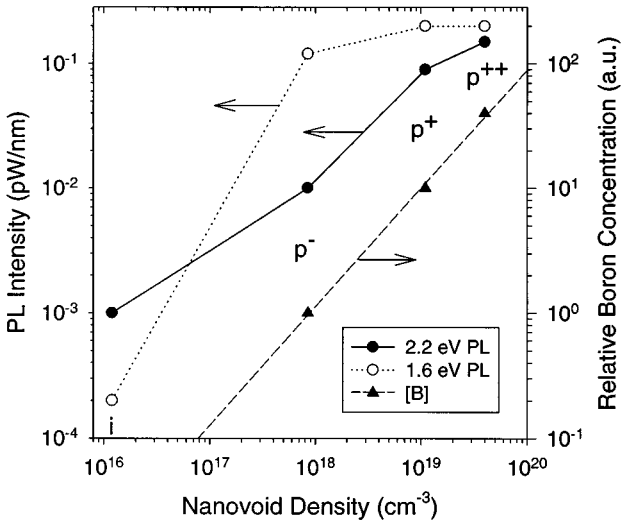

FIG. 12. Intensity of 1.6 (open circles) and 2.2 eV (filled circles) PL peaks from the porous layers of Fig. 3 as functions of nanovoid density of unetched *a*-Si:H layers as measured by small angle x-ray scattering. Nanovoid density and boron concentration have a nearly 1:1 correspondence, as shown by the relative gas phase boron concentrations from Table I (triangles, right axis).

etched layer becomes more rough for films with less boron. If nanovoid density does control pore density, then increasing layer porosity by varying etch conditions will create smaller *a*-Si:H structures. By our results, then, PL energy would be size independent. Further x-ray scattering and electron microscopy studies comparing unetched and etched films would be helpful.

Addition of carbon to the *a*-Si:H films results in an increase in band gap of the unetched film and an increase in PL energy of the porous film. From this finding, we see two possibilities: (1) at least one of the two radiative states (electron or hole) in the red emission is a conduction or valence band state, or (2) different carbon concentrations result in etching differences, which may cause variations of structure size or surface chemistry. Like boron, carbon also increases nanovoid density.[18] It seems reasonable that the general decrease in PL intensity with increased carbon content, as seen in Figs. 10 and 11, is due to higher defect densities in the films with more carbon.

The strong correlation of 2.2 eV PL intensity with boron concentration in Fig. 12 may indicate that this PL peak originates from boron-related states, possibly boron oxides. Alternatively, the 2.2 eV PL may be affected by structural differences in the porous layer due to the higher nanovoid densities in films with high boron content. As for the $\sim$1.6 eV PL, all evidence points to discrete surface states as its origin. First, it is composed of multiple sharper peaks within the broad peak. Second, oxidation, which should primarily modify the surface layer, reduces 1.6 eV PL intensity. Finally, its energy or intensity does not appear to be dependent on structure size.

V. CONCLUSIONS

We have observed room temperature red-orange light emission from anodized porous *a*-Si:H and *a*-Si:C:H films, clearly demonstrating that crystallinity is not a requirement for light emission. Luminescent porous layers were produced over a range of boron doping concentrations. No red emission was observed from phosphorous-doped *n*-type *a*-Si:H films. We see clear evidence of multiple PL processes with broad peaks at $\sim$1.5–1.6 and $\sim$2.2 eV. We find no evidence for size-dependent PL from porous *a*-Si:H as the PL peak energy was not affected by variations in layer porosity. The intensity of PL peak at $\sim$2.2 eV correlates well with boron concentration and nanovoid density in the starting *a*-Si:H film. We propose that anodic pore formation is seeded on nanovoids in the *a*-Si:H layer. PL from anodized p^+*a*-Si:H shows considerable temperature-dependent structure in its spectra, which is consistent with discrete defect or impurity states playing a role in the radiative process. Investigation of PL energy versus band gap energy of porous *p*-type *a*-Si:C:H films revealed a close correlation between the two. These data support the surface defect model for the $\sim$1.6 eV PL.

ACKNOWLEDGMENTS

We are indebted to E. Bustarret for useful discussions and to Materials Research Group, Inc. for use of the cryostat. M. Estes gratefully acknowledges the support of the Air Force Institute of Technology through the Civilian Institute Fellowship Program. We acknowledge partial support from the National Science Foundation Engineering Research Center grant ECD9015128 and from the Colorado Advanced Technology Institute.

[1] E. Bustarret, M. Ligeon, and L. Ortéga, Solid State Commun. **83**, 461 (1992).
[2] E. Bustarret, J. Cali, Y. Cros, M. Brunel, I. Mihalcescu, and M. Ligeon, J. Non-Cryst. Solids **164–166**, 937 (1993).
[3] E. Bustarret, M. Ligeon, and M. Rosenbauer, Phys. Status Solidi B **190**, 111 (1995).
[4] S. Lazarouk, S. Katsuba, N. Kazuchits, G. D. Cesare, S. L. Monica, G. Maiello, E. Proverbio, and A. Ferrari, in *Microcrystalline and Nanocrystalline Semiconductors*, edited by L. Brus, M. Hirose, R. W. Collins, F. Koch, and C. C. Tsai (Materials Research Society, Pittsburgh, 1994), Vol. 358, p. 93.
[5] X.-M. Bao and H.-Q. Yang, Appl. Phys. Lett. **63**, 2246 (1993).
[6] A. I. Yakimov, N. P. Stepina, A. V. Dvurechenskii, and L. A. Scherbakova, Physica B **205**, 298 (1995).
[7] K. H. Jung, S. Shih, D. L. Kwong, C. C. Cho, and B. E. Gnade, Appl. Phys. Lett. **61**, 2467 (1992).
[8] K. Higa, T. Asano, and T. Miyasato, Jpn. J. Appl. Phys. **33**, L1733 (1994).
[9] M. S. Brandt, H. D. Fuchs, M. Stutzmann, J. Weber, and M. Cardona, Solid State Commun. **81**, 307 (1992).
[10] Y. Kanemitsu, K. Suzuki, S. Kyushin, and H. Matsumoto, Phys. Rev. B **51**, 13 103 (1995).
[11] W. E. Carlos and S. M. Prokes, J. Appl. Phys. **78**, 2129 (1995).
[12] S. M. Prokes, W. E. Carlos, and O. J. Glembocki, Phys. Rev. B **50**, 17 093 (1994).
[13] B. H. Augustine, E. A. Irene, Y. J. He, K. J. Price, L. E. McNeil, K. N. Christensen, and D. M. Maher, J. Appl. Phys. **78**, 4020 (1995).
[14] T. Tiedje, in *Materials Issues in Applications of Amorphous Silicon Technology*, edited by D. Adler, A. Madan, and M. J. Thompson (Materials Research Society, Pittsburgh, 1985), Vol. 49, p. 121.
[15] T. Tiedje, B. Abeles, and B. G. Brooks, Phys. Rev. Lett. **54**, 2545 (1985).
[16] M. J. Estes and G. Moddel, Appl. Phys. Lett. **68**, 1814 (1996).
[17] Z. N. Lu, D. J. Lockwood, and J.-M. Baribeau, Nature (London) **378**, 258 (1995).
[18] D. L. Williamson, Mater. Res. Soc. Symp. Proc. **377**, 251 (1995).
[19] J. I. Pankove, in *Encyclopedia of Physical Science and Technology* (Academic, New York, 1987), p. 647.

[20] R. E. Hollingsworth, M. J. Estes, C. DeHart, and P. K. Bhat, presented at *American Vacuum Society* 41st *National Symposium*, Denver, CO (American Vacuum Society, New York, 1994).
[21] E. Bustarret, (private communication).
[22] R. W. Collins, M. A. Paesler, and W. Paul, Solid State Commun. **34**, 833 (1980).
[23] L. T. Canham, Appl. Phys. Lett. **57**, 1046 (1990).
[24] Y. H. Seo, K. S. Nahm, M. H. An, E.-K. Suh, Y. H. Lee, K. B. Lee, and H. J. Lee, Jpn. J. Appl. Phys. **33**, 6425 (1994).
[25] J. von Behren, K. B. Ücer, L. Tsybeskov, J. V. Vandyshev, and P. M. Fauchet, J. Vac. Sci. Technol. B **13**, 1225 (1995).
[26] J. C. Vial, A. Bsiesy, F. Gaspard, R. Hérino, M. Ligeon, F. Muller, R. Romestain, and R. M. Macfarlane, Phys. Rev. B **45**, 14 171 (1992).
[27] R. A. Street, in *Semiconductors and Semimetals*, edited by J. Pankove (Academic, New York, 1984), Vol. 21B, p. 197.
[28] M. J. Estes, PhD dissertation, Department of Electrical Engineering, University of Colorado, 1995.
[29] D. W. Cooke, B. L. Bennett, E. H. Farnum, W. L. Hults, K. E. Sickafus, J. F. Smith, J. L. Smith, T. N. Taylor, P. Tiwari, and A. M. Portis, Appl. Phys. Lett. **68**, 1663 (1996).
[30] J. Lin, L. Z. Zhang, Y. M. Huang, B. R. Zhang, and G. G. Qin, Appl. Phys. Lett. **64**, 3282 (1994).
[31] G. Moddel and B. Wilner (unpublished).
[32] S. M. Prokes, J. Mater. Res. **11**, 305 (1996).